

## CHITOSAN-COPPER PAINT TYPES AS ANTIFOULING

MARCIA HEUSER<sup>1</sup>, AND GALO CÁRDENAS<sup>1,2\*</sup>

<sup>1</sup>Centro de Biomateriales y Nanotecnología, Universidad del BíoBío,  
Av. Collao 1202, CP 4051381, Concepción, Chile.

<sup>2</sup>Quitoquímica Ltda, LAM, Golfo de Arauco 3666, Parque Industrial Coronel, Coronel.

### ABSTRACT

A prototype of antifouling paints was prepared with a Qs-Cu (I)-Fe (II) complex as a possible replacement for traditional antifouling net paints, which contain a large concentration of copper, finding them in an order of 10-30 % depending on the company, and either in water or solvent based. A Qs-Cu complex was prepared, with a solution at 3% with acetic acid, and then Fe<sub>2</sub>O<sub>3</sub> was added to the solution. FT IR analysis was carried out, as well as analysis of the TGA at the Qs and the complex with Qs-Cu, and with the solution, three different paints were prepared. Those that varied volume of diethylene glycol added to them. The analysis of the paints was carried out, once the paint was pervaded in a network of polyamide, through SEM with EDX and TEM, which was purchased with the commercial paints, water based and solvent based. One of the objectives is to be able to compare the coverage of the network with the commercial paint, and that of the complex Qs-Cu. The results showed that the best paint obtained was paint #2, found to be similar to that pervaded with water based paint.

**Keywords:** antifouling, chitosan complex, net paints

### INTRODUCTION

To decrease the “fouling” effect (the phenomenon of accumulation of an elevated biodiversity of opportunist organisms) on the nets used for the cultivation of trout and salmon, a series of antifouling paints have been formulated (1-7). The principal is based on a thin layer of antifouling paint, whose composition is a biocide. On the submerged surface, a thin cap of a solution, this is toxic for the early phases of the organisms that make up the fouling, forms by dissolving (8). The composition, abundance and seasonality of the fouling depend on geographic factors such as water temperature, salinity, lighting, tides, and turbidity, among other things (9). There are organisms that colonize marine installations in their first life stages or larval stages, where they move freely by the water column in search of a substrate to settle down on. Then, these communities begin to develop, increasing their weight and size, which causes the following consequences: Increase of the solid area on the net, which decreases the flow of water thorough it by 30 to 40% (2, 10), which therefore creates an increase in the resistance to currents and a change in the conditions within the cage, reducing the O<sub>2</sub>(g) levels and increasing the ammonium levels, produced by the decomposition of organic material (11).

Antifouling paints are basically made up of: a binding body or matrix, active compound, auxiliary compounds and solvent. These products are only formulated with a cuprous oxide such as biocide, its leaching is in smaller quantities, and therefore, it does not affect the salmon or the area surrounding the cages (12). The matrix or the binding body of the antifoulings determines the velocity with which the biocide particles will be released from the active component. The velocity of leaching or detachment of the toxic agent is a critical factor that influences the efficiency of the coating, it should sufficiently high to provide protection, but not excessively high, which would reduce the duration of the coating, and elevate the releasing in the marine environment (13).

The antimicrobial activity of chitosan is unstable and sensitive to many factors such as molecular weight. Recent investigations showed that low molecular weight chitosan exhibited strong bactericidal activities compared to chitosan with high molecular weight. Since chitosan degradation can be caused by the coordinating bond, we attempt to synthesize and characterize the chitosan-Cu (II) complex, and thereafter study the coordinating bond effect on its antibacterial activity against *Salmonella enteritidis*(14).

One of the big problems of salmon farming is the growth of aquatic fungi, which makes up one of the most frequent mycosis in fresh water fish. Three orders (*Saprolegniales*, *Leptomitales* y *Feronosporales*) of the class *Oomycetes* includes species that can infect the fish, those belonging to the *Saprolegniaceae* family being the most pathogens (15). The species of the genus *Saprolegnia* have an accepted mycelium, very branched, with a cotton-like look under water. Its reproductive structures are separated from the somatic hyphas by

septum and the asexual reproduction is carried out by biflagellate zoospores produced by vegetative hyphas, which are mobile, and therefore facilitates their dispersion (16).

A general overview of marine paints, paying particular attention to the case of antifouling paints is described by Almeida et al (17). After locating these paints in the anticorrosive protection systems used on the underwater parts of ships and/or other moving structures, a summary is made of the main types of antifouling products used through history up to the present time. This is complemented by a systematic assessment of the main types of living organisms that fix themselves to the underwater parts of ships. Consideration is also briefly made of the main basic mechanism by which the different types of antifouling paints work.

For these reasons, we designed the synthesis of several paints based on Chitosan-Cu(I)-Fe(III) complexes which are biodegradable and with similar antifouling properties than the commercial paints in the market.

### EXPERIMENTAL

#### Materials

Chitosan was purchased from Quitoquímica Ltda. Its degree of deacetylation was 80% and its Mv was 103.900 g/mol, (16). Cuprous oxide was purchased from the Sigma-Aldrich Chemical Company. Acetic acid from Fisher Scientific Commercial. Iron trioxide was purchased from Sigma-Aldrich Chemical Company, diethylene glycol Merck-Schuchardt and ethanol 95% from Diprolab.

#### Preparation of the (complex Qs-Cu)

For the preparation of the complex 1:3 Qs-Cu, it was left in ethanol for twelve hours with constant stirring. It was then filtered and dried at 40°C (18).

#### Preparation of the Composite (Qs-Cu Paints)

The complex Qs-Cu (I) was weighed, and Fe<sub>2</sub>O<sub>3</sub> was added to avoid the oxidation of copper (I) to copper (II), acetic acid was added until it reached a capacity of 100 ml in constant stirring. From this solution, three different paints were prepared; paint #1, paint #2 and paint #3, which varied in volume (2, 3, 4ml) of diethylene glycol added, whose mix was stirred for 2 hours.

#### FT IR

Spectrophotometer FT IR Nicolet Magna Model 550 connected to a computer with OMNIC software for data processing. A pellet of KBr at 2% is prepared from each sample.

#### TGA

Perkin-Elmer equipment model TGA-7 with a temperature control microprocessor and a program of data for thermo analysis. They weigh between

3-5 mg and a warming program of 10°C /min from 25-550°C in an atmosphere of nitrogen was used (18).

**SEM Measurement**

The microstructure, morphology and the thickness of the film were imaged using a JSM6380LV-JEOL Scanning Electron Microscope; front and cross section micrographs were obtained from each sample, the micrographs were taken 5000X of magnification for the front side and between 1000X and 3000X of magnification for the cross section (19).

**TEM**

Electronic microscope of a JEOL 1200 EX II transmission of a 4 Å of resolution, equipped with an EDX Model Norell, which also allows analysis by electron diffraction (19).

**RESULTS AND DISCUSSION**

**FT-IR Analysis**

The medium spectrum is shown in figure 1 for Chitosan (fig. 1a) and chitosan copper complex (fig. 1b- 1c)

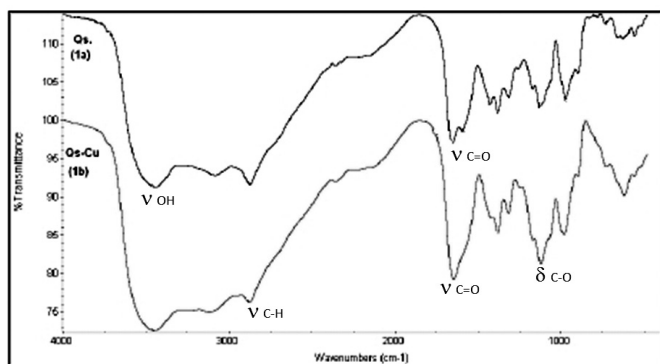


Fig.1.a Medium FT-IR spectrum of chitosan(Qs).

Figure 1.b Medium FT-IR spectrum of complex Qs-Cu.

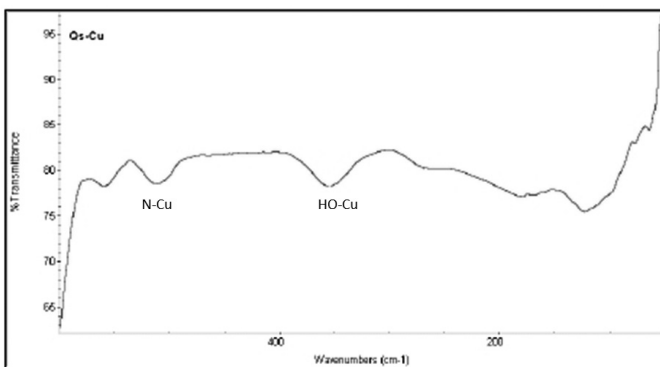


Figure 1.c Far FT-IR spectrum of Qs-Cu complex.

From fig 1.a in chitosan, it is possible to observe the existence of the complex formation between the copper ion with the NH<sub>2</sub> (C-2) group so as with the group OH (C-6) (22).

We can observe that the band assigned to NH<sub>2</sub> free group of chitosan change its absorbance when complex form with copper (compare the figures 1.b 1.c). The band at 355 related to δHO-Cu and δN-Cu at 443 in table 2 are the most important to observe the reaction of copper with chitosan.

**Table 1.** Assignment of band in FTIR spectra of chitosan and chitosan-copper mid range.

Band	Mode	Wavelength (cm <sup>-1</sup> )Qs.	Wavelength (cm <sup>-1</sup> )Qs-Cu
OH	Tension	3445	3451
CH	Tension	2920	2876
C=O (Amidel)	Tension	1520	1590
-NH <sub>2</sub> free	Flexion	1600	1597
-CH <sub>2</sub> -OH -CH	Deformation	1423 y 1380	1370 y 1252
-CO	Tension	1085	1090
NH (free amine)	Flexion	661	620

**Table 2.** Allocation of bands for FT-IR chitosan-copper.

Band	Type of vibration	Wavelength (cm <sup>-1</sup> )Qs-Cu
HO-Cu	Flexion	355
HN-Cu	Flexion	267
N-Cu	Flexion	443

**TGA**

The thermal stability of the paints were measured by TGA.

**Table 3.** The thermal stability data of the paints prepared.

Sample	Temperature Initial decomposition	Decomposition temperature maximum	Final Temperature (mass remaining)
Temperature and Percentage Mass remanent			
Qs	262,21 °C (91,09%)	315°C (70%)	540,24°C (38,1%)
Qs-Cu BPM	233,83 °C (92,98%)	310°C (82%)	510,99 °C (51,41%)
Paint 1 BPM	75,56 °C (98,94 %)	162,5°C (60%)	591,12 °C (12,04%)
Paint 2BPM	75 °C ( 98% )	145°C (60%)	590 °C (8,721%)

No great variations are observed in the thermogravimetric analysis carried out on Paint 1 BPM and Paint 2 BPM, this analysis was not carried out for 3 BPM.

**SEM Analysis**

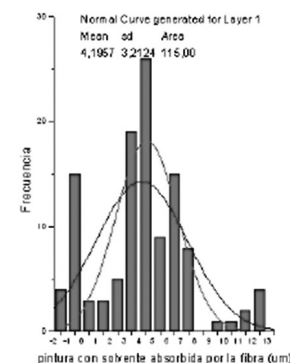
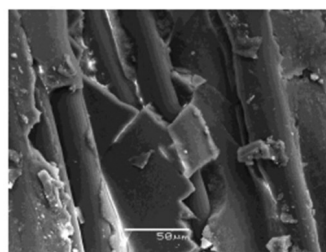


**Figure 2.** SEM Micrographs, the net impregnated with commercial paint solvent, and their respective histogram.

Table 4 shows the diameter of the points absorbed by the fibers on the net.

**Table 4.** Amount of paint absorbed in the nets.

Fishnet paint	Diameter painting absorbed $\phi$ ( $\mu\text{m}$ )
solvent paint	4,19
water paint	7,75
1 BPM Paint	-
2 BPM Paint	8,25
3 BPM Paint	2,41

Table 5 identifies the elements that constitute the solvent paint, water paint and Qs-Cu (I) and in table 5 percentage of the atomic for copper and iron in samples across SEM, for the spectrum a greater percentage of atomic copper and iron is presented.

With the SEM analysis, the form in which the paint absorbed by the net could be observed. It could be said that among the commercial paints, the water based paint with a measurement of 7.75  $\mu\text{m}$  in the fiber presents the best impregnation, as this is impregnated on the fiber in a homogeneous way, unlike the solvent based paint with a measurement of 4.19  $\mu\text{m}$  in the fiber (see fig 2), which begins to chip once dried. The three paints carried out with the Qs-Cu complex of BPM were absorbed by the fiber, observed through the micrographs a greater penetration in the fiber by paints #2 and #3. In paint # 1 an impregnation in the form of piles on the fiber was observed, therefore, in this case, how much paint was absorbed by the fiber was not analyzed. In the case of paint #2, it presented an average penetration in the fiber of 8.25  $\mu\text{m}$ , and in the case of paint #3, an average penetration in the fiber of 2.41  $\mu\text{m}$ . Therefore, paint #2 has the greatest penetration power, followed by the commercial water based paint.

Table 5 shows the percentage of atomic elements Cu and Fe, in samples obtained through EDX.

**Table 5.** Metal composition of net paints.

Paint	Diameter painting absorbed element $\phi$ ( $\mu\text{m}$ )	Atomic %
solvent paint	Cu	1.07
	Fe	0.74
water paint	Cu	0.13
	Fe	0.06
N° 1 BPM paint	Cu	3.32
	Fe	3.04
N° 2 BPM paint	Cu	0.38
	Fe	1.59
N° 3 BPM paint	Cu	1.88
	Fe	0.57

With the EDX analysis, it can be said that no paint, neither commercial nor that prepared with the Qs-Cu complex, homogeneously impregnate the net, which could be explained by the fact that no paint is completely homogenous and also the fibers exhibit some differences.

#### TEM Analysis

The analysis by TEM was carried out at  $\text{Cu}_2\text{O}$  (Fig. 3.a) and at  $\text{Fe}_2\text{O}_3$ , (Fig. 3.b), both electron diffraction and transmission micrograph, are able to determine the size and shape of the particles and therefore be able to see how the compounds are mainly found in the Qs-Cu paints. It is observed that the  $\text{Fe}_2\text{O}_3$  particles have a smaller size compared to the  $\text{Cu}_2\text{O}$ .

Electron micrography was carried out on paints #1, #2 and #3 of the Qs-Cu complex of BPM to obtain particle size and its morphology.

The images show the different shapes and sizes of the particles. Micrographies were obtained, in order to prove if the size and morphology of the particles are homogenous.

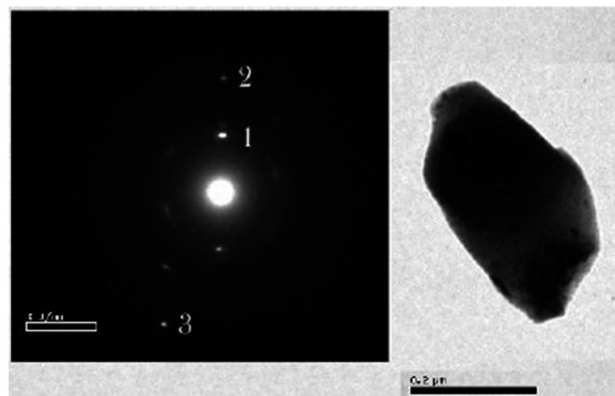


**Figure 3a.** Electron diffraction for  $\text{Cu}_2\text{O}$  with its respective transmission micrography.

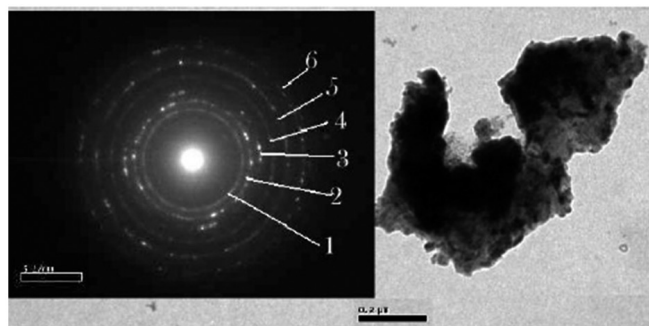
**Table 6.** Analysis of data provided by electron diffraction, and their comparison with tabulated data for Cu and Fe particles.

Compound	Ring	d hkl experimental (nm)	d hkl theoretical (nm)**	Planes hkl**
$\text{Cu}_2\text{O}$	1	0.2455	0.2465	111
$\text{Cu}_2\text{O}$	2	0.260	0.213	200
$\text{Cu}_2\text{O}$	3	0.122	0.12325	222
$\text{Fe}_2\text{O}_3$	1	0.2432	0.2519	110
$\text{Fe}_2\text{O}_3$	2	0.2060	0.2079	202
$\text{Fe}_2\text{O}_3$	3	0.1788	0.18428	024
$\text{Fe}_2\text{O}_3$	4	0.1492	0.14873	214
$\text{Fe}_2\text{O}_3$	5	0.1260	0.12595	220
$\text{Fe}_2\text{O}_3$	6	0.1071	0.11042	226

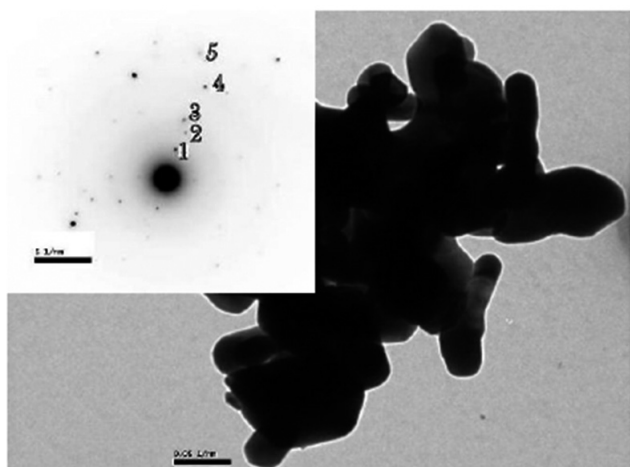
(\*\* JCPDS 1997)(22).

The analyses of the diffraction either in  $\text{Cu}_2\text{O}$  or  $\text{Fe}_2\text{O}_3$  reveals a good proximity of the experimental compared with tabulated data for crystallographic planes. Since is a paint the crystallinity is not quite relevant.

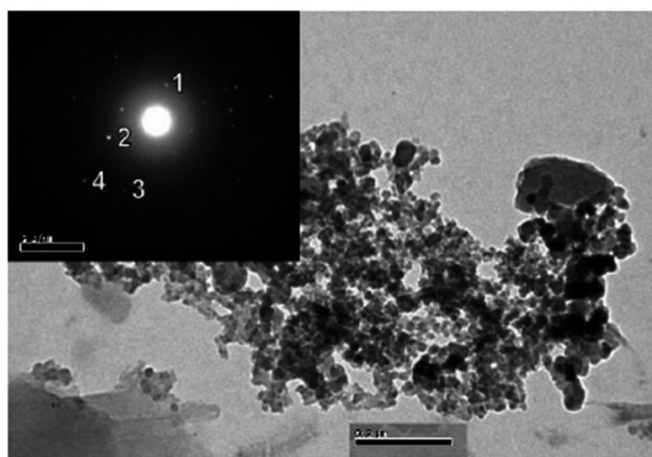
The figures 3b and c showed the electron diffraction of  $\text{Fe}_2\text{O}_3$  and paint #1 BPM and also their respective TEM.



**Figure 3b.** Electron diffraction for  $\text{Fe}_2\text{O}_3$  with its respective transmission micrography.

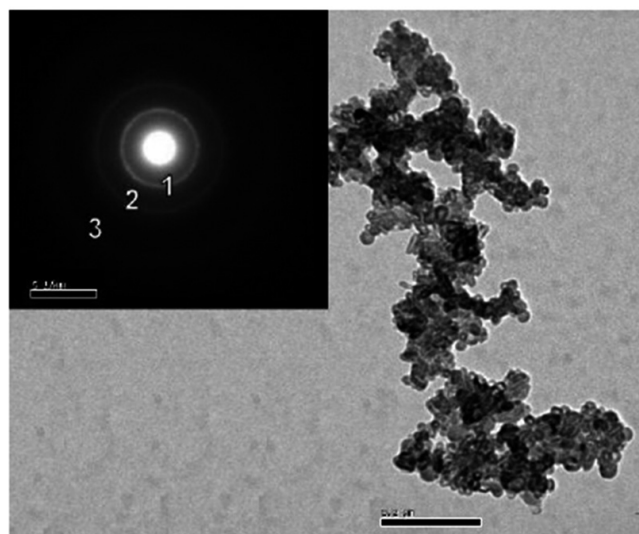


**Figure 3c.** Electron diffraction for paint #1 BPM with its respective transmission micrography.



**Figure 3d.** Electron diffraction for paint #2 BPM with its respective transmission micrography.

After the analysis of the data it is possible to summarize the planes from the electron diffraction data (see table 7).



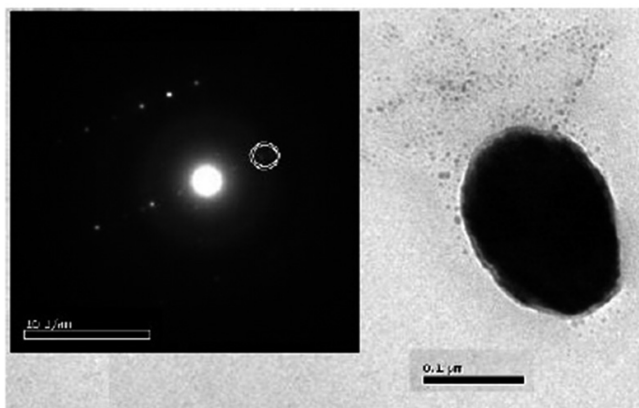
**Figure 3e.** Electron diffraction for paint #3 BPM with its respective transmission micrography.

Table 7 summarizes the data for all the paints.

**Table 7.** Analysis of data provided by electron diffraction, and their comparison with tabulated data for Cu and Fe in the paint.

Paint	Ring	d hkl experimental (nm)	d hkl theoretical (nm)**	Planes hkl**	Compound
1BPM	1	0.3810	0.36855	012	Fe <sub>2</sub> O <sub>3</sub>
1BPM	2	0.2291	0.2295	006	Fe <sub>2</sub> O <sub>3</sub>
1BPM	3	0.1812	0.1842	024	Fe <sub>2</sub> O <sub>3</sub>
1BPM	4	0.1135	0.1141	226	Fe <sub>2</sub> O <sub>3</sub>
1BPM	5	0.0874	N.E.*	N.E.*	N.E.*
2BPM	1	0.3524	0.36855	012	Fe <sub>2</sub> O <sub>3</sub>
2BPM	2	0.3509	0.36855	012	Fe <sub>2</sub> O <sub>3</sub>
2BPM	3	0.1658	0.16966	116	Fe <sub>2</sub> O <sub>3</sub>
2BPM	4	0.2356	0.2311	111	Fe <sub>2</sub> O <sub>3</sub>
3BPM	1	0.3524	0.36855	012	Fe <sub>2</sub> O <sub>3</sub>
3BPM	2	0.2096	0.2079	202	Fe <sub>2</sub> O <sub>3</sub>
3BPM	3	0.1216	0.12595	220	Fe <sub>2</sub> O <sub>3</sub>

\* N.E: It does not exist. (\*\* JCPDS 1997)



**Figure 3f.** Electron diffraction for commercial water based paint with its respective transmission micrography.

After the analysis, the average particle size is of 0.05  $\mu$ m.

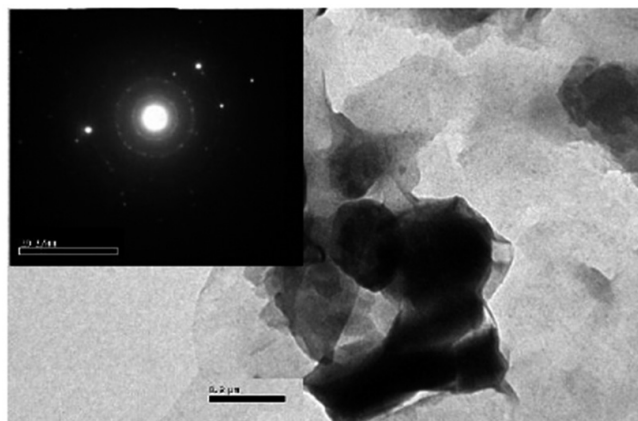


**Figure 3g.** Electron diffraction for commercial solvent based paint with its respective transmission micrography.

The analysis of the average size of the particles ends up being of 0.02  $\mu\text{m}$ .

**Table 8.** Particle size of  $\text{Cu}_2\text{O}$  and  $\text{Fe}_2\text{O}_3$ .

Compound	Particle size ( $\mu\text{m}$ )
$\text{Cu}_2\text{O}$	25.54
$\text{Fe}_2\text{O}_3$	4.53

The analysis of the oxides was carried out in a liquid phase; the liquid phase was carried out with acetic acid. The particle size of paint #1 of BPM is of 15.31  $\mu\text{m}$ ; comparing these particles with the  $\text{Cu}_2\text{O}$  and  $\text{Fe}_2\text{O}_3$  particles, it could not be known with certainty of which particles it is principally made up of, as the particle size of the oxides is not found within a range, rather than a unique value. Electron diffraction was carried out, which indicated that the paint is composed of oxide particles of iron, as deduced by the values of d hkl practical and theoretical (23).

The following table summarizes the particle size of the paints under study.

**Table 9.** Particle Size of the Paints Components.

Paint	Particle size ( $\mu\text{m}$ )
N° 1 BPM Paint	15.31
N° 2 BPM Paint	3.31
N° 3 BPM Paint	1.39
Solvent Paint	0.02
Walter Paint	0.05

Particle size of the BPM paints is a factor that influences the penetration of the paint in the fiber, as a smaller size of particles in the paint would benefit in the sense that the paint would penetrate the fiber much easier, which is better, as it facilitates a better impregnation of the paint in the fiber. Perhaps for this reason, the water based commercial paint has good penetration in the fiber. No such data is available on commercial paints such as: Flexabard, Biodeg, Seaguard, Kelcot, Norimp and others, in which only the percentage of  $\text{Cu}_2\text{O}$  and  $\text{Fe}_2\text{O}_3$  are given.

## CONCLUSIONS

1. The initial decomposition temperature of the complexes Qs-Cu (I) BPM and Qs-Cu (I) APM, occur at 233 and 248° C, with a remaining mass of 92% and 94 % respectively at that temperature. In contrast, paint #1 BPM and 2 BPM both have an initial decomposition temperature of 75 °C, with a remaining mass at this temperature of 98 %. These differences are due to the paints with low molecular weight containing diethylene glycol, and by being laminating made the polymer lower its meeting point and decomposition temperature of the components of fusion.

2. According to the FT-IR range carried out at the Qs-Cu (I) complex and at the Qs, it could be proven that there is formation of complexes between the groups  $\text{NH}_2$  and OH of the Qs with the Cu (I).

3. In scanning electronic microscopy (SEM), it was observed that the paint that best impregnated the net was paint #2 of BPM, as, unlike the other paints, it is absorbed by the fiber and not covered by layers. According to the size of paint #3, it should penetrate more, but it is observed in Table 4 that it penetrates less than 1/3 than paint #2. This is because they have a smaller particle size.

4. In transmission electronic microscopy (TEM), through electron diffraction, it was concluded that the paints of low molecular weight are mainly made up of iron, which would indicate that there would be a better impregnation of paint in the fiber, as the particles of iron oxide are of a smaller size than those of copper, which facilitates the net point impregnating the net with greater ease through impregnated physical adsorption of the  $\text{Fe}_2\text{O}_3$  that does not form part of the complex.

5. According to the analysis carried out and the obtained results in this report, it is concluded that the best antifouling paint is paint #2 of BPM due to the better ratio Cu/Fe and better absorption in the net fiber.

## ACKNOWLEDGEMENTS

The authors would like to thank the financial support of Fondef DO 4I-1286 Project and the scholarship granted to M. Heuser.

## REFERENCES

1. Aquanoticias. July 2003. N° 79. Vol. 15.
2. Beveridge M.C. 1991. Cage Aquaculture. Fishing News Books. 351 pp.
3. Bruno, D.W. and Stamps, D.J. (1987). J. Fish Dis.,10: 513- 517.
4. Portillo, E. (2002). Bol. Inst. Esp. Oceanogr.18 (1-4) 401-440.
5. Kennish M. J. 1997. Heavy Metals, Chapter 6. In: Estuarine and marine Pollution. Institute of Marine and Coastal Sciences, Rutgers University, New Jersey. 524.
6. Langvad, F. 1994. K. in Norwegian Fish Farming. In: G. J. Mueller, ed., Salmon *Saprolegniasis*. Bonneville Power Administration, Div. Fish and Wildlife, Portland, OR. pp 188-201.
7. Lorentzen M.; Maage, A.; Julshamn,K. 1998. Aquaculture Nutrition. 4: 67-72.
8. Lovegrove T. 1979. Fish Farming International. 33-37.
9. Willoughby S.1999. Environment Requirements and Consequences of Fish Farming, in: Manual of Salmonid Farming. Fishing New Books. Great Britain. 61- 66.
10. Solver T. 1994. Environmental testing of fishnet antifoulants. Final Report. Terra Miljo Laboratorium S.A. 14.
11. Pazian B. 2004. Water base antifouling net treatments. Flexabar-Aquatech Corporation. En: El Periódico de Acuicultura. N°8; pag.20.
12. Milne P.H. 1970. Mar. Res.,1, 31 .
13. Noga, E.J. (1996). Fish Diseases, Diagnosis and Treatment. Mosby- Year Book, 565pp.
14. Mekahlia, S.; Bouzid, B., Physics Procedia 2(3), 1015-1053 (2009).
15. Padgett, D. E. 1984. *Mycology* 76: 372-375.
16. Roberts, R.J. (1981). Patología de los peces , Bailliere Tyndall, London. 336.
17. Almeida, E. Diamantino, T.C., De Souza, O., Progress in Organic Coating 59 (1), 2-20 (2007).
18. Neira K (2003). Síntesis y caracterización de quitosano a partir de quitina extraída de langostino rojo (*pleuroncodes monodom*). Estudio de su capacidad de retención de colesterol *in vitro* mediante derivados con aminoácidos. Tesis para optar al título de Químico Marino. Univ. Católica de la Santísima Concepción, 12-17 (2008).
19. Skoog, D A & West D N (1979). Fundamentos de Química Analítica. Ed. Reverté, S.A. 413-417.
20. Chiessi, E., Paradosi, G., Venanzi, M. Pispisa, B. Int. J. Biol. Macromol. 15, 145 (12993).
21. Domard, A., Int. J. Biol. Macromol. 9, 333 (1987)
22. (a)Taboada, E. A.. Tesis para optar al grado de Doctor en Ciencias con Mención Química. 32-35 (2003). (b) Taboada, E., Cárdenas , G., J. Chil. Chem. Soc. 54, 1-5 (2009).
23. Powder diffraction file, Inorganic phases JCPDS 1997, International center for diffraction data, Pennsylvania, USA.